

## Original Article

# MicroRNA-205 inhibits the apoptosis of renal tubular epithelial cells via the PTEN/Akt pathway in renal ischemia-reperfusion injury

Wu Chen\*, Yuan Ruan\*, Sheng Zhao, Jinzhuo Ning, Ting Rao, Weimin Yu, Xiangjun Zhou, Cong Liu, Yucheng Qi, Fan Cheng

*Department of Urology, Renmin Hospital of Wuhan University, Wuhan 430000, Hubei, P. R. China. \*Equal contributors.*

Received June 11, 2019; Accepted November 30, 2019; Epub December 15, 2019; Published December 30, 2019

**Abstract:** Renal ischemia-reperfusion injury (IRI) is the main cause of acute kidney injury (AKI). Many studies on renal IRI have been performed recently, but effective treatments are still lacking. Evidence exists that small endogenous noncoding RNAs are involved in the ischemia-reperfusion process. This article aims to investigate whether microRNA-205 (miR-205) is involved in this process and to determine its role in the hypoxia-induced injury of renal tubular epithelial cells (TECs). We found that miR-205 was significantly downregulated in rats with renal IRI and in HK-2 cells with hypoxia-reoxygenation injury (HRI) in vitro. In vitro, overexpression of intracellular miR-205 by transfection of a miR-205 mimic significantly reduced apoptosis, and this antiapoptotic effect was antagonized by a miR-205 inhibitor. Moreover, we confirmed that PTEN is a target of miR-205. miR-205 exerted its protective effect by inhibiting HK-2 cell apoptosis and promoting HK-2 cell proliferation by inhibiting the expression of PTEN during HRI, and this protective effect was blocked by silencing PTEN. Therefore, we confirmed that miR-205 may target the PTEN/Akt signaling pathway to alleviate hypoxia-induced renal cell damage. miR-205 may be a new potential target for the treatment of renal IRI.

**Keywords:** MiR-205, renal ischemia-reperfusion injury, apoptosis, PTEN/Akt

## Introduction

Renal ischemia-reperfusion injury (IRI) is one of the main causes of acute kidney injury (AKI) and has a clinical incidence of approximately 5% and a mortality rate of 50%-80% [3]. Even when patients recover from the initial injury, renal IRI may still have long-term effects, such as chronic kidney disease, on patients [4]. IRI is common during shock, sepsis, and kidney transplantation, and the pathogenesis of IRI is thought to involve intracellular calcium overloading, massive oxygen free radical accumulation, and microcirculatory disorders. Studies have shown that the loss of functional tubular epithelial cells (TECs) via apoptosis plays an important role in renal IRI [7, 8]. Despite that many studies that have been performed on renal IRI, effective treatments are still lacking.

MicroRNAs (miRNAs) are single-stranded non-coding RNA molecules that range in length

from 21-25 nucleotides. Studies have shown that miRNAs can regulate gene expression by inhibiting protein translation or targeting mRNA for degradation by binding to their target mRNA [9]. In this way, miRNAs play important roles in proliferation, differentiation, and apoptosis [10, 11] and are therefore thought to potentially play important regulatory roles in the development of various diseases. After decades of research, miRNAs have been shown to contribute to the development of various kidney diseases. For example, miR-21 and miR-22 have been shown to be key regulators of renal fibrosis [12, 13], while miR-192, miR-93 and miR-29c have been shown to be involved in the development of diabetic nephropathy [14-16]. Moreover, miR-21, miR-34a, miR-200c and miR-215 have all been shown to be potential biomarkers or therapeutic targets for renal cell carcinoma [17-19]. miRNAs play a key role in regulating renal IRI. Studies have shown that miR-205 induces significant changes in the ischemic injury of the

gracilis muscle in rats [20]. Our previous study showed that miR-205 was significantly down-regulated during renal IRI, and the same results were observed in HK-2 cells subjected to hypoxia-reoxygenation (H/R) treatment. However, the role and mechanism of miR-205 in renal IRI remains to be studied. Therefore, we herein aimed to investigate the role of miR-205 in renal IRI and explore its molecular mechanism.

### Materials and methods

#### *Animals*

Sprague-Dawley rats (4-5 weeks of age) weighing 180-220 g were purchased from the Center of Experimental Animals at Wuhan University Medicine College (Hubei, China). All rats were caged in a standard temperature-controlled room with an alternating 12-h light/dark cycle and had free access to water and a standard laboratory diet. The study was approved by the Wuhan University Committee on Ethics for Animal Experiments. All rats were randomly divided into two groups, the sham group and the surgical group (n = 6).

#### *Renal I/R model*

The rats were fasted overnight and anesthetized with an intraperitoneal injection of 3% sodium pentobarbital (0.1 ml/100 g body weight), and an abdominal incision was made. An electric heating pad was used to keep the rat body temperature constant. In the IRI group, the renal pedicles were dissected and clamped with nontraumatic clamps for 30 minutes [1]. The renal pedicles were then orthotopically reconstituted for 24 hours, after which the rats from the experimental group were euthanized by decapitation, and their kidney tissues were carefully dissected for subsequent experiments. In the sham control group rats, an abdominal incision was made, but the renal pedicles were not clamped. Each group contained six rats.

#### *Cell culture and hypoxia-reoxygenation (H/R) treatment*

This experiment utilized HK-2 cells cultured in high-glucose DMEM supplemented with 10% fetal bovine serum, penicillin (100 U/ml), and streptomycin (100 U/ml). To simulate an anoxic

environment, the cells were cultured in a three-gas incubator containing 94% N<sub>2</sub>, 5% CO<sub>2</sub> and 1% O<sub>2</sub> for 24 hours followed by reoxygenation (5% CO<sub>2</sub>, 21% O<sub>2</sub>, and 74% N<sub>2</sub>) for 12 hours. The cells were then harvested for RNA isolation, protein extraction and many other experiments.

#### *Cell transfection*

The miR-205 mimic, scramble construct, anti-miR-205, phosphatase and tension homolog (PTEN)-siRNA and their corresponding negative controls (NCs) were purchased from RiboBio (Ribo, China). After reaching 60-70% confluence, HK-2 cells were transfected with the mimic, inhibitor and scramble mentioned using Lipofectamine 3000 (Life Technologies, USA) according to the manufacturer's protocol.

#### *Histopathological examination*

The obtained kidney tissues were fixed in 4% formalin for 24 hours, dehydrated, and then embedded in paraffin according to conventional protocols. Then, 4- $\mu$ m-thick paraffin sections were stained with hematoxylin and eosin. The histological findings were scored using the semiquantitative scoring system developed by Paller [2]. In this system, the following scores are used: (1) TEC smoothness, 1; (2) loss of the brush-like edge, 2; (3) cytoplasmic vacuolization, 1; (4) cell necrosis, 1 or 2; and (5) obstruction of the tubular lumen, 1 or 2. With this scoring method, a maximum score of seven points can be obtained. To ensure the objectivity of the results, the sections were evaluated by a pathologist who was blinded to the groupings.

#### *TUNEL staining*

To explore renal cell apoptosis induction by IRI, an in situ apoptosis assay kit (Promega, USA) was used. The TUNEL assay was performed according to the manufacturer's instructions. Briefly, the obtained tissue samples were fixed overnight in a 4% paraformaldehyde/phosphate buffered saline (PBS, pH 7.4) solution at 4°C. After washing three times with 1 $\times$  PBS solution, the samples were immersed in 70% ethanol at 20°C for at least 24 hours. After thoroughly washing three times with 1 $\times$  PBS, the samples were immersed in permeabilization buffer on ice for 15 minutes and then washed with PBS. Subsequently, the samples were incubated wi-

th 50 ml of reaction buffer (5 ml of TdT enzyme + 45 ml of labeling safe buffer) at 37°C for 90 minutes. The labeling process was terminated by washing with PBS solution. Cell counting was performed under a light microscope, and the degree of cell apoptosis was expressed as the percentage of positive cells.

### *Immunohistochemical (IHC) staining*

Rat tissues were fixed in 10% neutral-buffered formalin and embedded in paraffin for immunohistochemistry analysis. Samples were cut into 5- $\mu$ m-thick sections, deparaffinized in xylene, and rehydrated using a decreasing ethanol gradient followed by 0.1 M PBS. The tissues were then sequentially blocked with 0.3% hydrogen peroxide in methanol for 15 minutes and with 5% goat serum in PBS for 30 minutes at room temperature. The tissue sections were first incubated with the primary antibody p-Akt (1:100, Cell Signaling Technology, Ser473) or PTEN (1:200, Cell Signaling Technology, 138G6) in 1% goat serum at 4°C overnight. The slides were then sequentially incubated with a biotinylated anti-rabbit secondary antibody (Vector Laboratories) for 1 hour and with horseradish peroxidase streptavidin (Vector Laboratories, SA-5004) for 30 minutes at room temperature before being visualized with a DAB kit (Vector Laboratories, SK-4100). The slides were subsequently counterstained with 5% (w/v) Harris hematoxylin. Finally, sections were counterstained with hematoxylin and observed by two independent pathologists. The percentage of stained target cells was evaluated in 10 random microscopic fields per tissue section, and their averages were subsequently calculated.

### *Immunofluorescence (IFC) staining*

Cryosections (10  $\mu$ m) of rat kidneys were fixed in 4% paraformaldehyde. After washing with PBS, the sections were incubated with a primary p-Akt (1:400, Cell Signaling Technologies, Ser473) or PTEN (1:100, Abcam, Y184) antibody at 4°C overnight. Then, the sections were incubated with the appropriate fluorescein-labeled IgG for 1 hour and washed with PBS; nuclei were stained blue with 5  $\mu$ g/ml DAPI (4',6-diamidino-2-phenylindole, Beyotime, Nantong, China) for 2 minutes. A fluorescence microscope was used to assess the expression of PTEN and p-Akt.

### *Quantitative real-time polymerase chain reaction (qRT-PCR)*

Total RNA was extracted from cells using the mirVana kit (Ambion, Austin, TX) and then reverse transcribed into cDNA using a Takara RNA PCR kit (Takara Biotechnology, Dalian, China). The TaqMan miRNA assay kit (Applied Biosystems) was used to detect the relative expression of miR-205. The small nuclear RNA U6 was used as an internal control to normalize the expression of miR-205. Finally, the  $2^{-\Delta\Delta C_t}$  values were used to calculate the fold change.

### *Luciferase reporter assay*

The PTEN 3'UTR carrying a miR-205 binding site was constructed by PCR and subsequently cloned into the pMIR-REPORT vector to construct the wild-type PTEN (PTEN-WT) luciferase reporter construct. Then, the PTEN-WT construct and miR-205 mimic or scrambled sequence oligonucleotides were cotransfected into HK-2 cells using Lipofectamine 3000 (Life Technologies, USA). Lysates were harvested after 36 hours, and luciferase activity was measured using the dual-luciferase assay (Promega, Madison, WI, USA). All procedures were performed according to the manufacturer's instructions.

### *Western blot analysis*

The cells were resuspended in RIPA lysis buffer (Solarbio, Beijing, China) containing 0.1 mM PMSF and a protease inhibitor (Roche). After 30 minutes of lysis on ice, lysates were collected by centrifugation at 12,000 rpm for 20 minutes at 4°C. The supernatant was collected and subjected to 12% SDS-PAGE, and the proteins were then transferred to PVDF membranes. The samples were incubated in their respective primary antibodies at 4°C overnight. After rinsing three times with TBS-T, the membranes were incubated with a horseradish peroxidase-labeled secondary antibody for 1 hour at 37°C. The Western blot bands were scanned using the Odyssey Infrared Imaging System (LI-COR Biosciences, Lincoln, NE, USA), and quantitative analysis was performed using Odyssey v1.2 software (LI-COR Biosciences, Lincoln, NE, USA). The experiment was repeated three times for each group.

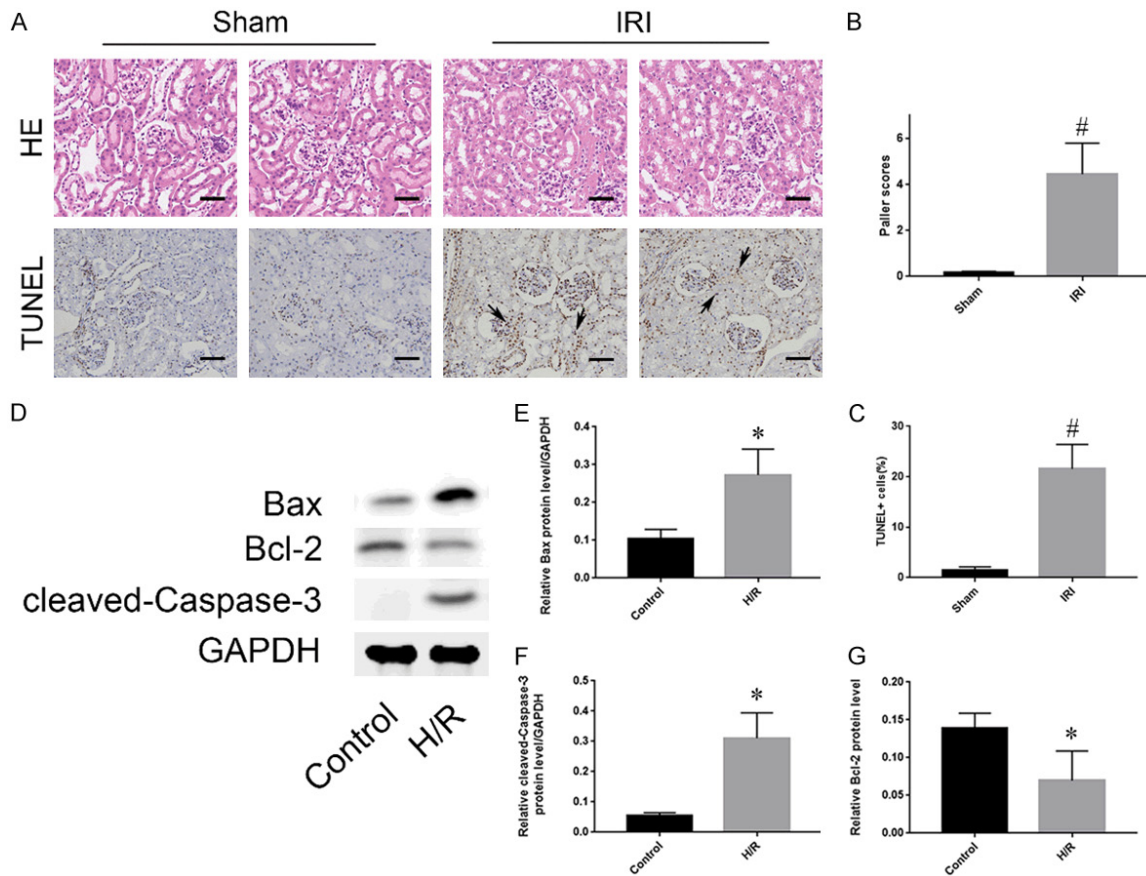


**Figure 1.** IRI induces renal apoptosis. A: HE and TUNEL staining of kidney tissues from the sham and IRI groups. The brown-black cells indicated by the black arrows are TUNEL positive. Scale bar, 50  $\mu$ m. B: Evaluation of Paller scores after HE staining in the sham and IRI groups under an optical microscope. C: Comparison of the percentage of TUNEL-positive cells in the sham and IRI groups. D: Expression levels of apoptosis-related proteins (Bax, Bcl-2 and cleaved caspase-3) in the control and H/R groups. E-G: Quantitative values of the relative expression levels of the Bax, Bcl-2 and cleaved caspase-3 proteins in the control and H/R groups. The data are expressed as the mean  $\pm$  SD. #P < 0.05 versus the sham group, \*P < 0.05 versus the control group.

#### Apoptosis assay

HK-2 cells were seeded in 6-well plates. After reaching 80% confluence, the cells were digested with trypsin without EDTA, washed twice with cold PBS and resuspended in buffer. Double staining with Annexin V-fluorescein isothiocyanate (FITC) and propidium iodide (PI) was performed using an Annexin V-FITC/PI apoptosis detection kit (BD Pharmingen, Beijing, USA) according to the manufacturer's instructions. Subsequently, flow cytometry (BD FACS Calibur, USA) was used to detect and quantify the apoptotic cells.

#### Statistical analysis

The experimental data are presented as the mean  $\pm$  standard deviation (SD). The significance of differences between data was evaluated

using one-way analysis of variance (ANOVA) with SPSS 19.0 statistical software (SPSS Inc., Chicago, IL), and P < 0.05 was considered significant. All graphs shown in this manuscript were constructed with GraphPad Prism 5.0 software. The experimental data were obtained from three experimental replicates.

#### Results

##### Renal IRI induces apoptosis

To investigate the cytopathological changes during renal IRI, Sprague-Dawley rats were selected to establish a renal IRI model and divided into an experimental group (IRI group) and a sham operation group (sham group) [1]. In the IRI group, renal perfusion was restored for 24 hours after the kidney pedicles were

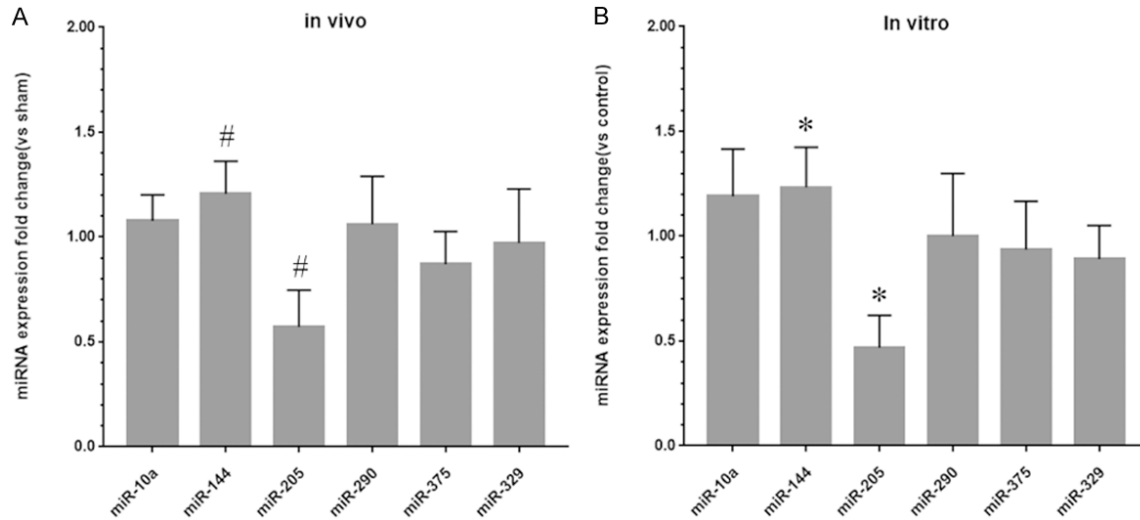


**Figure 2.** miR-205 is significantly downregulated in IRI kidney tissues and HK-2 cells subjected to H/R treatment. A: Fold changes in the expression levels of miR-10a, miR-144, miR-205, miR-290, miR-375 and miR-329 in the IRI group compared to the sham group. B: Fold changes in the expression levels of miR-10a, miR-144, miR-205, miR-290, miR-375 and miR-329 in the H/R group compared to the control group. The data are expressed as the mean  $\pm$  SD. #P < 0.05 versus the sham group, \*P < 0.05 versus the control group.

clamped for 30 minutes, and the rats in the control group underwent only the sham operation. Kidney samples from the IRI and sham groups were collected and stained with hematoxylin and eosin. The rats subjected to renal IRI showed more pronounced renal pathological damage than rats in the sham group (**Figure 1A**). The main features were tubular cell swelling, widespread tubular dilation degeneration, nuclear condensation, and inflammatory cell infiltration. The Paller scores of the IRI group were also significantly higher than those of the sham group (**Figure 1B**). When TUNEL-stained kidney tissues were observed by light microscopy, the number of apoptotic cells in the IRI group was significantly increased compared with that in the sham group (**Figure 1A, 1C**). Moreover, in vitro, HK-2 cells were cultured in an anoxic environment to simulate ischemia within the tissue, and proteins from the HK-2 cells treated with or without H/R were collected. Western blot analysis showed that the protein expression levels of apoptosis-related markers such as caspase-3 and Bax in the H/R group were significantly higher than those in the control group (**Figure 1D**). Together, these results showed that the degrees of renal injury and TEC apoptosis were significantly increased in the IRI group compared with those in the control group.

#### *Hypoxia inhibits miR-205 expression in HK-2 cells*

To further examine the role of microRNAs in renal IRI, qRT-PCR was used to detect the levels of microRNAs that are potentially involved in the development of renal IRI, including miR-10a, miR-144, miR-205, miR-290, miR-375 and miR-329, in both normal and IRI kidney tissues. The level of miR-205 was significantly decreased in IRI kidney tissues. In addition, the level of miR-144 was increased, and the changes in the other four miRNAs were not statistically significant (**Figure 2A**). This result was subsequently verified in HK-2 cells subjected to H/R in vitro (**Figure 2B**).

#### *Role of miR-205 in renal IRI*

To further investigate the role of miR-205 in hypoxia-induced renal cell injury, a miR-205 mimic or inhibitor was transfected into HK-2 cells under hypoxic conditions, and the transfection efficiency was confirmed by qRT-PCR (**Figure 3A**). The level of miR-205 was significantly upregulated in cells transfected with the miR-205 mimic. Moreover, subsequent flow cytometry analyses revealed that the number of apoptotic cells in the mimic group was lower than that in the H/R group. In contrast, the inhibitor of miR-205 further aggravated hypox-

MicroRNA-205 alleviates renal ischemia-reperfusion injury

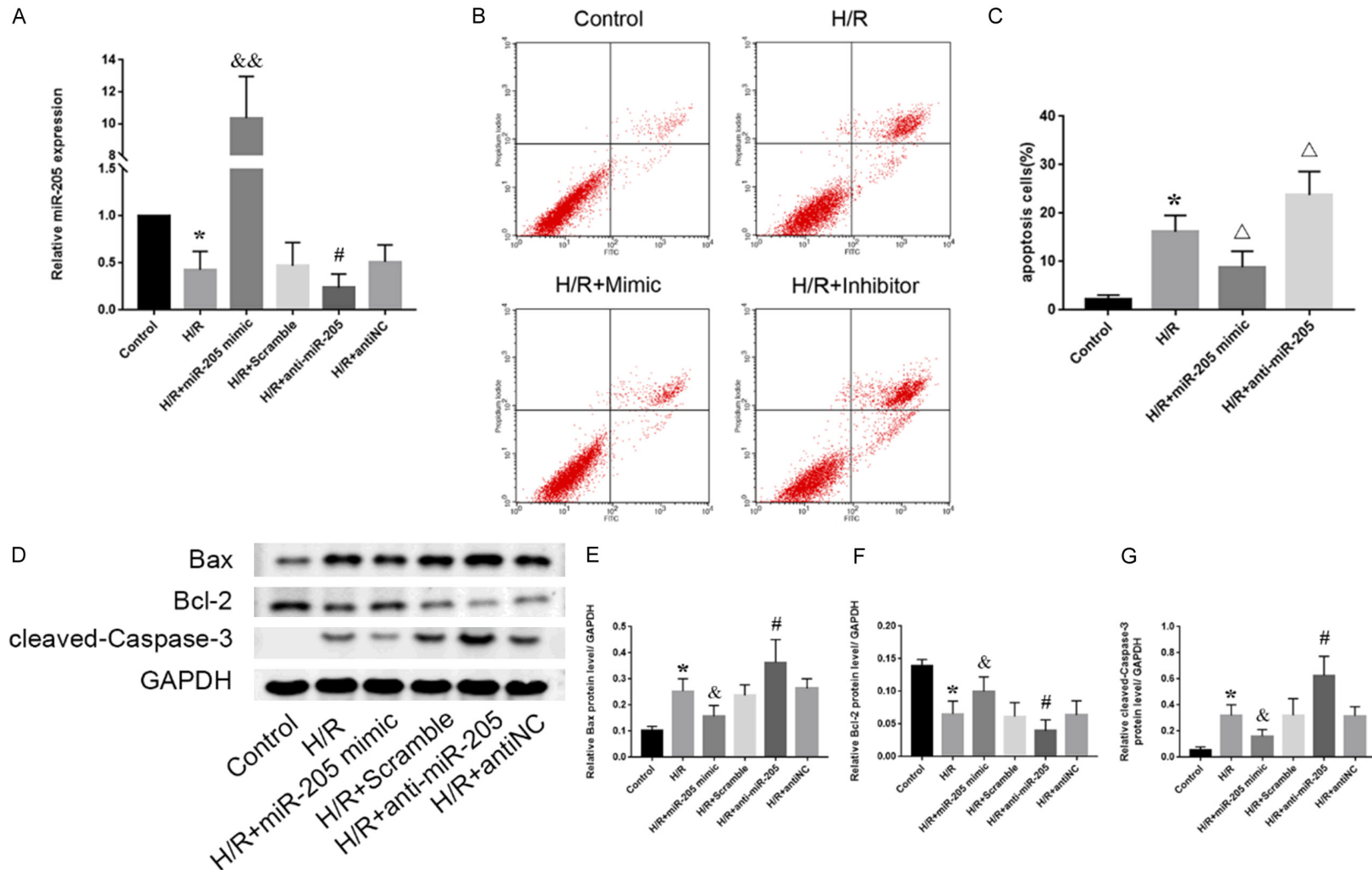


**Figure 3.** Hypoxia can inhibit the expression of miR-205 in HK-2 cells, while overexpression of miR-205 can reduce the expression of apoptosis-related proteins and attenuate hypoxia-induced apoptosis. A: Expression of miR-205 in HK-2 cells subjected to H/R after transfection with a mimic or inhibitor. B: Flow cytometry analysis of the effect of mimic or inhibitor transfection on HK-2 cell apoptosis. C: Quantitative analysis of the percentage of apoptotic cells by flow cytometry. D: Expression levels of apoptosis-related proteins (Bax, Bcl-2 and cleaved caspase-3). E-G: Quantitative values of the relative expression levels of the Bax, Bcl-2 and cleaved caspase-3 proteins. The data are expressed as the mean  $\pm$  SD. \*P < 0.05 versus the control group, &P < 0.05 and &&P < 0.01 versus the H/R + scramble group, #P < 0.05 versus the H/R + antiNC group,  $\Delta$ P < 0.05 versus the H/R group.

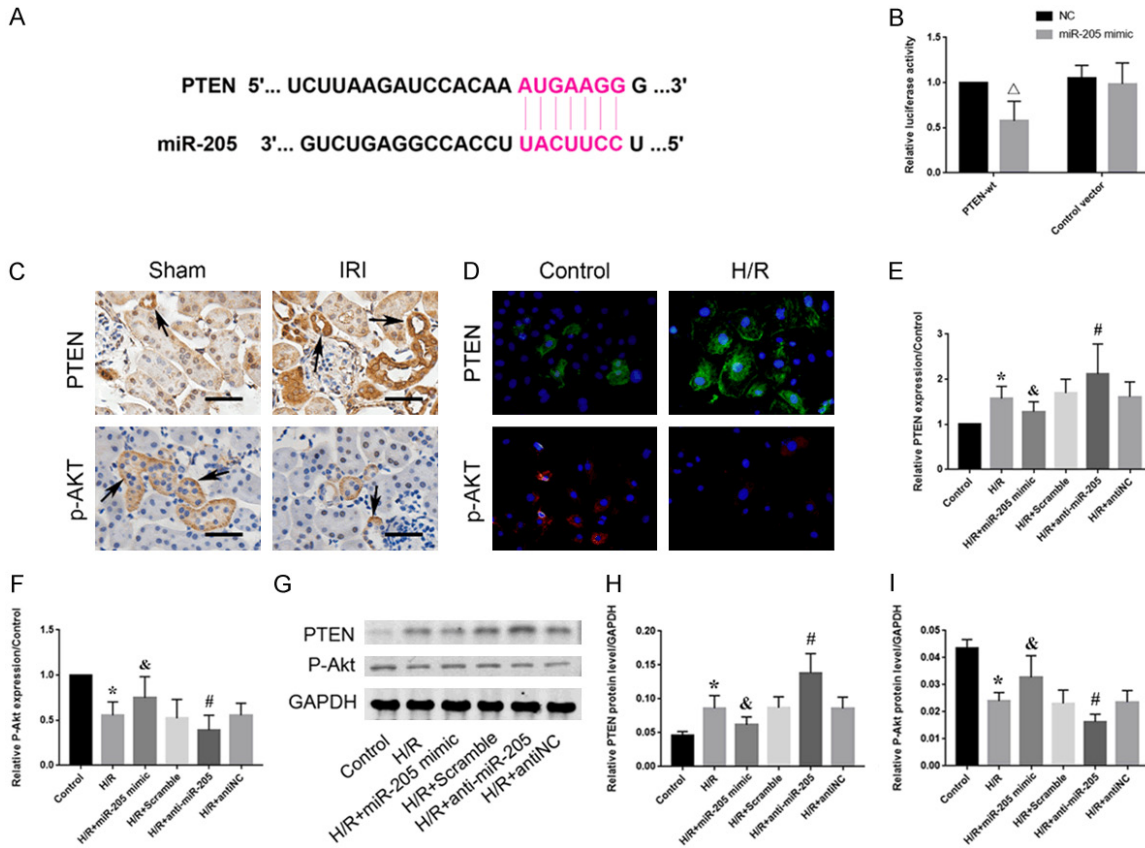


**Figure 4.** miR-205 directly targets PTEN in HK-2 cells during HRI. **A:** A gene database predicted a conserved binding site for miR-205 in the 3'-UTR of the PTEN gene. **B:** A wild-type PTEN (PTEN-WT) luciferase reporter construct carrying the PTEN 3'UTR or control vector was cotransfected into HK-2 cells with miR-205 mimic or scramble, and luciferase activity was measured. **C:** Immunohistochemistry analysis of the PTEN and p-Akt protein expression levels in kidney tissues from normal rats and rats subjected to renal IRI. The brown cells indicated by the black arrow are positively stained. Scale bar, 50  $\mu$ m. **D:** Immunofluorescence staining of PTEN and phosphorylated Akt. HK-2 cells were stained to assess the effect of H/R on PTEN (green) and p-Akt (red). Original magnification, 400 $\times$ . **E:** Expression levels of PTEN-related mRNAs compared to those in the control group. **F:** Expression levels of p-Akt-related mRNAs compared to those in the control group. **G:** Expression levels of proteins related to PTEN and p-Akt. **H, I:** Quantitative analysis of the expression levels of proteins related to PTEN and p-Akt. The data are expressed as the mean  $\pm$  SD. \*P < 0.05 versus the control group, &P < 0.05 versus the H/R + scramble group, #P < 0.05 versus the H/R + antiNC group,  $\Delta$ P < 0.05 versus the control group.

ia-induced apoptosis (**Figure 3B, 3C**). We conclude that overexpression of miR-205 can significantly protect proximal tubular cells from apoptosis in renal IRI. Subsequently, Western blot analysis was used to further validate the role of miR-205 in renal IRI at the protein level (**Figure 3D**). After hypoxia-induced cell injury, the cellular expression of apoptosis-related proteins was significantly enhanced. However, this phenomenon was obviously different in the mimic group. Overexpression of miR-205 significantly reduced the expression levels of cleaved caspase-3 and Bax/Bcl-2, whereas inhibition of miR-205 enhanced the expression of apoptosis-related proteins (**Figure 3D**). In conclusion, miR-205 can attenuate hypoxia-

induced renal injury by inhibiting renal cell apoptosis.

#### The PTEN/Akt pathway is the target of miR-205 during HRI/IRI

To further investigate the possible mechanism of miR-205 action during HRI, a series of experiments were performed to verify the relationship between miR-205 and the PTEN/Akt pathway. Computer analyses confirmed that the 3'-UTR of the PTEN gene was the conserved binding site of miR-205 (**Figure 4A**). To verify the relationship between miR-205 and PTEN, a wild-type PTEN (PTEN-WT) luciferase reporter construct carrying the PTEN 3'UTR was con-

## MicroRNA-205 alleviates renal ischemia-reperfusion injury

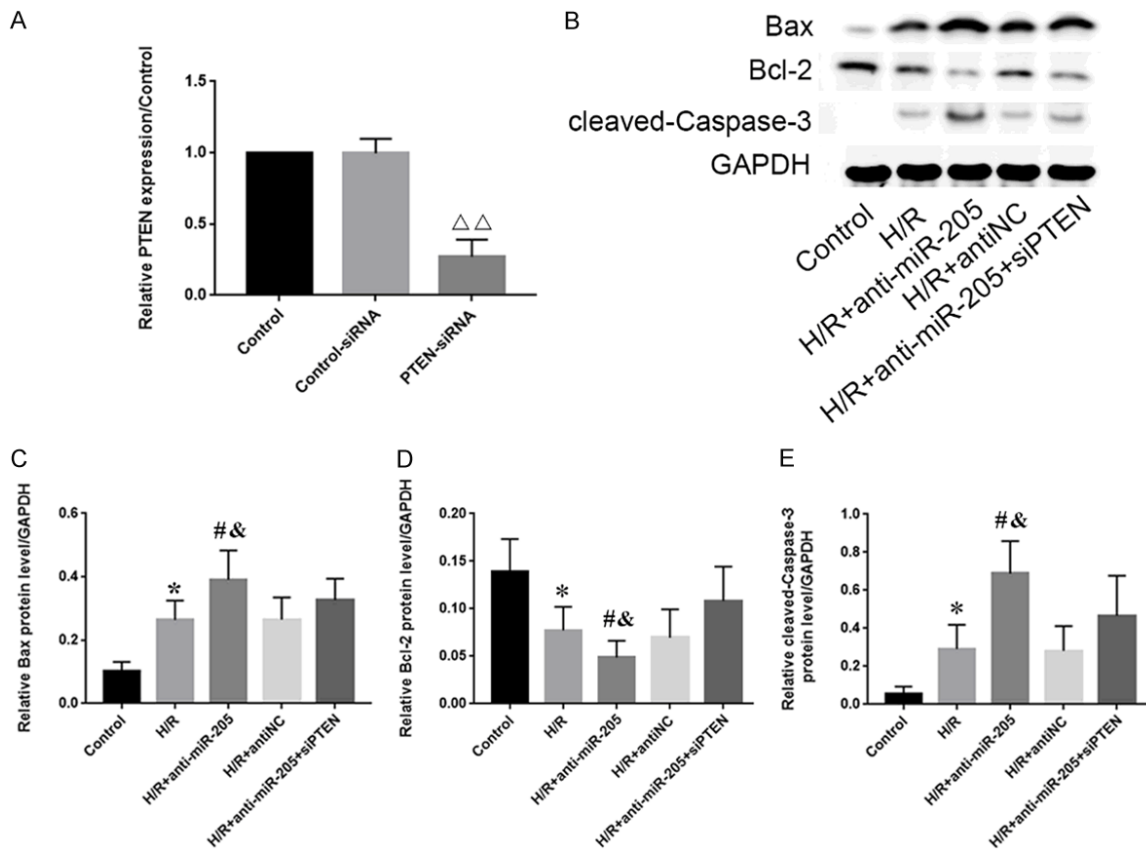


**Figure 5.** Silencing PTEN can reverse hypoxia-induced apoptosis during HRI by enhancing the inhibitory effect of miR-205. A: Expression of PTEN mRNA in HK-2 cells after transfection with control-siRNA or PTEN-siRNA. B: Differences in apoptosis-related proteins (Bax, Bcl-2 and cleaved caspase-3) between the H/R + anti-miR-205 + siPTEN and H/R + anti-miR-205 groups as determined by Western blot analysis. C-E: Quantitative values of the relative protein expression of Bax, Bcl-2 and cleaved caspase-3. The data are expressed as the mean  $\pm$  SD.  $\Delta\Delta P < 0.01$  versus the control-siRNA group, \* $P < 0.05$  versus the control group, # $P < 0.05$  versus the H/R + antiNC group, & $P < 0.05$  versus the H/R + anti-miR-205 + siPTEN group.

structured. After the transfection of a miR-205 mimic or inhibitor with PTEN-WT into HK-2 cells subjected to H/R, luciferase activity was measured. Compared to that in the control group, the luciferase activity in the group transfected with the miR-205 mimic was lower. However, the inhibition of miR-205 reversed this effect (Figure 4B). In addition, kidney tissues from normal rats and rats subjected to renal IRI were subjected to immunohistochemical analyses to evaluate the protein expression of PTEN and p-Akt (Figure 4C). The percentage of PTEN-positive cells was significantly increased in the IRI group, while the percentage of cells positively stained for p-Akt was downregulated. Immunofluorescence analyses of PTEN and p-Akt in HK-2 cells showed the same results as those obtained using immunohistochemistry (Figure 4D). Moreover, after hypoxic injury, the protein

expression level of PTEN was decreased significantly and p-Akt was upregulated in the mimic group. In contrast, the downregulation of PTEN and upregulation of p-Akt were reversed upon transfection of the inhibitor into HK-2 cells (Figure 4G-I). Consistent with the Western blot results, the qRT-PCR results confirmed the mRNA expression trends (Figure 4E, 4F). These results indicate that the PTEN/Akt pathway is a direct target of miR-205.

### *Silencing PTEN can enhance the protective effect of miR-205 during HRI*

After HK-2 cells were transfected with control-siRNA or PTEN-siRNA, qPCR was used to detect PTEN expression at the mRNA level. PTEN mRNA expression was significantly downregulated in the PTEN-siRNA group, whereas the

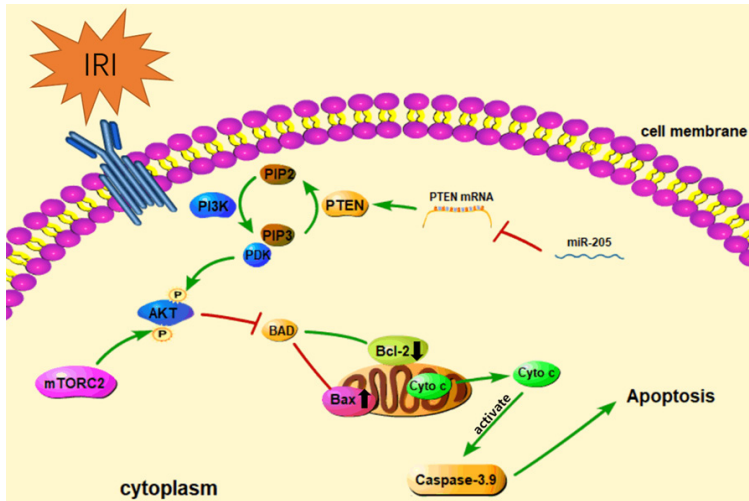


**Figure 6.** Schematic diagram of the involvement of miR-205 in HK-2 cell apoptosis during renal IRI. During renal IRI, the expression of miR-205 in HK-2 cells is significantly downregulated, which reduces the inhibitory effect on PTEN. The enhancement of PTEN expression induces a shift from PIP3 to PIP2, which decreases the local concentration of PIP3 and inhibits the recruitment of PDK1. The activation of Akt is inhibited by a decrease in PDK1, thus reducing the inhibition of BAD by activating Akt. An increase in the Bax/Bcl-2 ratio promotes mitochondrial outer membrane permeabilization (MOMP) and leads to the mitochondrial release of numerous cytochromes and activation of the caspase cascade, which eventually leads to apoptosis.

expression level in the control-siRNA group did not significantly differ from that in the control group (**Figure 5A**). Subsequently, an inhibitor and/or siPTEN were cotransfected into HK-2 cells subjected to H/R treatment to verify whether PTEN/Akt is the pathway via which miR-205 plays a protective role in HRI. The expression levels of apoptosis-related proteins were significantly increased after HRI, and this phenomenon was more pronounced in the inhibitor group. Contrary to the above results, the expression levels of cleaved caspase-3 and Bax/Bcl-2 were significantly lower in the H/R + anti-miR-205 + siPTEN group than in the H/R + anti-miR-205 group (**Figure 5B**).

### Discussion

The renal IRI-induced loss of tubular cell function plays a key role in the development of AKI. Studies have shown that the apoptosis of renal tubular cells caused by the accumulation of oxygen free radicals and inflammatory reactions is one of the main causes of renal IRI [5-8]. In recent years, numerous studies have shown that the PTEN/Akt pathway is a key mediator of renal cell damage during renal IRI.

PTEN, located on chromosome 10, is a tumor suppressor gene and plays a key role in the development of different human tumors [21-24]. As a negative regulator of PI3K, PTEN can dephosphorylate and convert phosphatidylinositol-3,4,5-trisphosphate (PIP3) into phosphatidylinositol-4,5-diphosphate (PIP2) to reduce Akt activation and prevent Akt-regulated downstream signaling events (**Figure 6**), including cell growth and proliferation [25, 26].

The PI3K family is comprised of three main classes that have different structures and functions, with class I PI3Ks being the most widely studied. Class I PI3Ks are a family of heterodimeric enzymes that are composed of a regulatory subunit and a catalytic subunit. Multiple growth factors and signaling complexes can activate PI3Ks by binding to their membrane receptors. The phosphorylation of PIP2 is catalyzed by activated PI3K and converted to PIP3. As a second messenger, an increase in the local concentration of PIP3 may recruit a subset of pleckstrin homology (PH) domain-containing proteins, particularly the serine/threonine kinase Akt (also known as protein kinase B) and phosphatidylinositol-dependent kinase 1 (PDK1), to the plasma membrane. PIP3 promotes PDK1 to phosphorylate Akt, which is fully activated by the phosphorylation of mammalian target of rapamycin complex 2 (mTORC2). Activated Akt can activate multiple downstream targets, the most well-known of which are mTORC1, BAD, CASP9, various FOXO proteins, GSK3 $\beta$ , MDM2 and TSC1. Through these downstream targets, Akt can inhibit apoptosis and regulate cell growth and differentiation [27-30]. The main mechanism explored herein is the regulation of the Bcl-2 family by Akt. The Bcl-2 family is divided into the following three groups based on their primary functions: (1) antiapoptotic proteins (Bcl-2, Bcl-X<sub>L</sub>, Bcl-W, Mcl-1, and Bfl-1/A1), (2) proapoptotic pore-formers (Bax, Bak, and Bok) and

(3) proapoptotic BH3-only proteins (Bad, Bid, Bik, Bim, Bmf, Hrk, NOXA, PUMA, etc.) [31]. The Bcl-2 family of proteins controls cell death primarily through direct binding interactions that regulate MOMP. MOMP eventually leads to the massive release of cytochrome C in mitochondria and activation of the caspase cascade, leading to apoptosis [32-34]. The interaction between Bcl-2 family proteins, especially the dynamic balance between Bcl-2 and Bax, plays a crucial role in regulating apoptosis. Studies have shown that activated Akt binds to the 14-3-3 protein to form a BAD/14-3-3 interaction by phosphorylating Ser-112 and Ser-136 on BAD. This induced binding prevents the binding of BAD and Bcl-2, enhances the amount of free Bcl-2 and disrupts the balance between Bcl-2 and Bax, thereby exerting antiapoptotic effects [35].

Interestingly, as regulators of their target genes, miRNAs have been shown to participate in numerous cellular processes, including growth and proliferation, together with PTEN. Xu confirmed that miR-155 promotes cell proliferation and inhibits apoptosis by the PTEN signaling pathway in psoriasis [36]. In recent years, an increasing number of scholars have confirmed that PTEN also plays an important role in renal IRI [37]. In this experiment, the luciferase reporter assay confirmed that PTEN is a direct target of miR-205 and is negatively regulated by miR-205. Silencing PTEN with a small interfering RNA significantly attenuated the effect of miR-205 inhibition on the hypoxia-induced apoptosis of HK-2 cells. Moreover, the PI3K/Akt pathway in HK-2 cells subjected to H/R treatment was significantly activated after silencing PTEN. Overexpression of miR-205 enhances Akt expression and significantly attenuates hypoxia-induced apoptosis (**Figure 6**). Together, these findings suggest an important regulatory role of miR-205 in relieving renal IRI.

In this study, we first investigated the changes in miR-205 that occur during hypoxia-induced renal TEC damage. The results showed that miR-205 is significantly downregulated in kidney tissues subjected to IRI and in HK-2 cells subjected to HRI. Further analyses showed that overexpression of miR-205 can significantly reduce the hypoxia-induced apoptosis of HK-2 cells. On the other hand, inhibition of miR-205 can aggravate hypoxia-induced apoptosis. In the latest research, Chen found that MALAT1 can promote MPP+-induced neuronal apopto-

sis by downregulating miR-205-5p [38]. Moreover, Zhang found that miR-205 can inhibit renal cell apoptosis by targeting CMTM4 in patients with chronic kidney disease [39]. We provide evidence consistent with the findings of Zhang that overexpression of miR-205 is effective in reducing the hypoxia-induced apoptosis of HK-2 cells.

Nevertheless, related experiments, such as regulating the expression of miR-205 in animals, are still necessary, and experiments using PTEN knockout rats are also urgently needed. In conclusion, it is hypothesized that miR-205 can significantly protect kidney cells from apoptosis in renal IRI through the PTEN/Akt pathway.

### Acknowledgements

This work was supported by grants from the Natural Science Foundation of China (no. 81870471 and no. 81800617).

### Disclosure of conflict of interest

None.

**Address correspondence to:** Dr. Fan Cheng, Department of Urology, Renmin Hospital of Wuhan University, Wuhan 430000, Hubei, P. R. China. Tel: +86-13307105017; E-mail: Urology1969@aliyun.com

### References

- [1] Yokota N, Daniels F, Crosson J and Rabb H. Protective effect of T cell depletion in murine renal ischemia-reperfusion injury. *Transplantation* 2002; 74: 759-763.
- [2] Paller MS and Neumann TV. Reactive oxygen species and rat renal epithelial cells during hypoxia and reoxygenation. *Kidney Int* 1991; 40: 1041-1049.
- [3] Gill N, Nally JV Jr and Fatica RA. Renal failure secondary to acute tubular necrosis: epidemiology, diagnosis, and management. *Chest* 2005; 128: 2847-2863.
- [4] Venkatachalam MA, Weinberg JM, Kriz W and Bidani AK. Failed tubule recovery, AKI-CKD transition, and kidney disease progression. *J Am Soc Nephrol* 2015; 26: 1765-1776.
- [5] Linkermann A, Brasen JH, Himmerkus N, Liu S, Huber TB, Kunzendorf U and Krautwald S. Rip1 (receptor-interacting protein kinase 1) mediates necroptosis and contributes to renal ischemia/reperfusion injury. *Kidney Int* 2012; 81: 751-761.

## MicroRNA-205 alleviates renal ischemia-reperfusion injury

- [6] Arai S, Kitada K, Yamazaki T, Takai R, Zhang X, Tsugawa Y, Sugisawa R, Matsumoto A, Mori M, Yoshihara Y, Doi K, Maehara N, Kusunoki S, Takahata A, Noiri E, Suzuki Y, Yahagi N, Nishiyama A, Gunaratnam L, Takano T and Miyazaki T. Apoptosis inhibitor of macrophage protein enhances intraluminal debris clearance and ameliorates acute kidney injury in mice. *Nat Med* 2016; 22: 183-193.
- [7] Zhou Y, Cai T, Xu J, Jiang L, Wu J, Sun Q, Zen K and Yang J. UCP2 attenuates apoptosis of tubular epithelial cells in renal ischemia-reperfusion injury. *Am J Physiol Renal Physiol* 2017; 313: F926-F937.
- [8] Liu XJ, Tan Y, Geng YQ, Wang Z, Ye JH, Yin XY and Fu B. Proximal tubule toll-like receptor 4 expression linked to inflammation and apoptosis following hypoxia/reoxygenation injury. *Am J Nephrol* 2014; 39: 337-347.
- [9] Lee R, Feinbaum R and Ambros V. A short history of a short RNA. *Cell* 2004; 116 Suppl: S89-92.
- [10] Piccoli MT, Gupta SK and Thum T. Noncoding RNAs as regulators of cardiomyocyte proliferation and death. *J Mol Cell Cardiol* 2015; 89: 59-67.
- [11] Subramanyam D, Lamouille S, Judson RL, Liu JY, Bucay N, Derynck R and Blalock R. Multiple targets of miR-302 and miR-372 promote reprogramming of human fibroblasts to induced pluripotent stem cells. *Nat Biotechnol* 2011; 29: 443-448.
- [12] Zhong X, Chung AC, Chen HY, Meng XM and Lan HY. Smad3-mediated upregulation of miR-21 promotes renal fibrosis. *J Am Soc Nephrol* 2011; 22: 1668-1681.
- [13] Dey N, Das F, Mariappan MM, Mandal CC, Ghosh-Choudhury N, Kasinath BS and Choudhury GG. MicroRNA-21 orchestrates high glucose-induced signals to TOR complex 1, resulting in renal cell pathology in diabetes. *J Biol Chem* 2011; 286: 25586-25603.
- [14] Deshpande SD, Putta S, Wang M, Lai JY, Bitzer M, Nelson RG, Lanting LL, Kato M and Nataraajan R. Transforming growth factor-beta-induced cross talk between p53 and a microRNA in the pathogenesis of diabetic nephropathy. *Diabetes* 2013; 62: 3151-3162.
- [15] Long J, Wang Y, Wang W, Chang BH and Danesh FR. Identification of microRNA-93 as a novel regulator of vascular endothelial growth factor in hyperglycemic conditions. *J Biol Chem* 2010; 285: 23457-23465.
- [16] Long J, Wang Y, Wang W, Chang BH and Danesh FR. MicroRNA-29c is a signature microRNA under high glucose conditions that targets Sprouty homolog 1, and its in vivo knock-down prevents progression of diabetic nephropathy. *J Biol Chem* 2011; 286: 11837-11848.
- [17] Zhang A, Liu Y, Shen Y, Xu Y and Li X. miR-21 modulates cell apoptosis by targeting multiple genes in renal cell carcinoma. *Urology* 2011; 78: 474, e413-479.
- [18] Yu G, Li H, Wang J, Gumireddy K, Li A, Yao W, Tang K, Xiao W, Hu J, Xiao H, Lang B, Ye Z, Huang Q and Xu H. miRNA-34a suppresses cell proliferation and metastasis by targeting CD44 in human renal carcinoma cells. *J Urol* 2014; 192: 1229-1237.
- [19] Wang X, Chen X, Han W, Ruan A, Chen L, Wang R, Xu Z, Xiao P, Lu X, Zhao Y, Zhou J, Chen S, Du Q, Yang H and Zhang X. miR-200c targets CDK2 and suppresses tumorigenesis in renal cell carcinoma. *Mol Cancer Res* 2015; 13: 1567-1577.
- [20] Hsieh CH, Jeng JC, Jeng SF, Wu CJ, Lu TH, Liliang PC, Rau CS, Chen YC and Lin CJ. MicroRNA profiling in ischemic injury of the gracilis muscle in rats. *BMC Musculoskelet Disord* 2010; 11: 123.
- [21] Jefferies MT, Cox AC, Shorning BY, Meniel V, Griffiths D, Kynaston HG, Smalley MJ and Clarke AR. PTEN loss and activation of K-RAS and beta-catenin cooperate to accelerate prostate tumorigenesis. *J Pathol* 2017; 243: 442-456.
- [22] Li K, Li GD, Sun LY and Li XQ. PTEN and SHIP: impact on lymphatic metastasis in breast cancer. *J Cancer Res Ther* 2018; 14: S937-S941.
- [23] Ahmed MW, Kayani MA, Shabbir G, Ali SM, Shinwari WU and Mahjabeen I. Expression of PTEN and its correlation with proliferation marker Ki-67 in head and neck cancer. *Int J Biol Markers* 2016; 31: e193-203.
- [24] Zhang HM, Fan TT, Li W and Li XX. Expressions and significances of TTF-1 and PTEN in early endometrial cancer. *Eur Rev Med Pharmacol Sci* 2017; 21: 20-26.
- [25] Song MS, Salmena L and Pandolfi PP. The functions and regulation of the PTEN tumour suppressor. *Nat Rev Mol Cell Biol* 2012; 13: 283-296.
- [26] Jia M, Chen X, Liu J and Chen J. PTEN promotes apoptosis of H2O2 injured rat nasal epithelial cells through PI3K/Akt and other pathways. *Mol Med Rep* 2018; 17: 571-579.
- [27] Danielsen SA, Eide PW, Nesbakken A, Guren T, Leithe E and Lothe RA. Portrait of the PI3K/AKT pathway in colorectal cancer. *Biochim Biophys Acta* 2015; 1855: 104-121.
- [28] Zhang X, Tang N, Hadden TJ and Rishi AK. Akt, FoxO and regulation of apoptosis. *Biochim Biophys Acta* 2011; 1813: 1978-1986.
- [29] Makker A, Goel MM and Mahdi AA. PI3K/PTEN/Akt and TSC/mTOR signaling pathways, ovarian dysfunction, and infertility: an update. *J Mol Endocrinol* 2014; 53: R103-118.
- [30] Worby CA and Dixon JE. PTEN. *Annu Rev Biochem* 2014; 83: 641-669.

## MicroRNA-205 alleviates renal ischemia-reperfusion injury

- [31] Kale J, Osterlund EJ and Andrews DW. BCL-2 family proteins: changing partners in the dance towards death. *Cell Death Differ* 2018; 25: 65-80.
- [32] Tait SW and Green DR. Mitochondria and cell death: outer membrane permeabilization and beyond. *Nat Rev Mol Cell Biol* 2010; 11: 621-632.
- [33] Goldstein JC, Waterhouse NJ, Juin P, Evan GI and Green DR. The coordinate release of cytochrome c during apoptosis is rapid, complete and kinetically invariant. *Nat Cell Biol* 2000; 2: 156-162.
- [34] Albeck JG, Burke JM, Spencer SL, Lauffenburger DA and Sorger PK. Modeling a snap-action, variable-delay switch controlling extrinsic cell death. *PLoS Biol* 2008; 6: 2831-2852.
- [35] Datta SR, Dudek H, Tao X, Masters S, Fu H, Gotoh Y and Greenberg ME. Akt phosphorylation of BAD couples survival signals to the cell-intrinsic death machinery. *Cell* 1997; 91: 231-241.
- [36] Xu L, Leng H, Shi X, Ji J, Fu J and Leng H. MiR-155 promotes cell proliferation and inhibits apoptosis by PTEN signaling pathway in the psoriasis. *Biomed Pharmacother* 2017; 90: 524-530.
- [37] Gao S, Zhu Y, Li H, Xia Z, Wu Q, Yao S, Wang T and Yuan S. Remote ischemic postconditioning protects against renal ischemia/reperfusion injury by activation of T-LAK-cell-originated protein kinase (TOPK)/PTEN/Akt signaling pathway mediated anti-oxidation and anti-inflammation. *Int Immunopharmacol* 2016; 38: 395-401.
- [38] Chen Q, Huang X and Li R. lncRNA MALAT1/miR-205-5p axis regulates MPP(+)-induced cell apoptosis in MN9D cells by directly targeting LRRK2. *Am J Transl Res* 2018; 10: 563-572.
- [39] Zhang H, Zhang X, Yuan X, Wang L and Xiao Y. MicroRNA-205 inhibits renal cells apoptosis via targeting CMTM4. *Iran J Basic Med Sci* 2015; 18: 1020-1026.